Production of highly oxygenated organic molecules (HOMs) from trace contaminants during isoprene oxidation

Anne-Kathrin Bernhammer[1,2], Lukas Fischer[1], Bernhard Mentler[1], Martin Heinritzi[3], Mario Simon[3] and Armin Hansel[1,2]

[1]Institute for Ion and Applied Physics, University of Innsbruck, 6020 Innsbruck, Austria
[2]IONICON Analytik GmbH, 6020 Innsbruck, Austria
[3]Institute for Atmospheric and Environmental Sciences, Goethe University of Frankfurt, 60438 Frankfurt am Main, Germany

Correspondence to: A. Hansel (armin.hansel@uibk.ac.at)

Abstract.

During nucleation studies from pure isoprene oxidation in the CLOUD chamber at CERN we observed unexpected ion signals at m/z = 137.133 ($C_{10}H_{17}^+$) and m/z = 81.070 ($C_6H_9^+$) with the recently developed proton transfer reaction time-of-flight mass spectrometer (PTR3-TOF) instrument. The mass-to-charge ratios of these ion signals typically correspond to protonated monoterpenes and their main fragment. We identified two origins of these signals: First secondary association reactions of protonated isoprene with isoprene within the PTR3 reaction chamber and secondly [4+2] cycloaddition (Diels-Alder) of isoprene inside the gas bottle which presumably forms the favoured monoterpenes limonene and sylvestrene, as known from literature. Under our PTR3 conditions used in 2016 an amount (relative to isoprene) of 2 % is formed within the PTR3 reaction chamber and 1 % is already present in the gas bottle. The presence of unwanted cycloaddition products in the CLOUD chamber impacts the nucleation studies by creating ozonolysis products as corresponding monoterpenes, and is responsible for the majority of the observed highly oxygenated organic molecules (HOMs). In order to study NPF from pure isoprene oxidation under atmospheric relevant conditions, it is important to improve and assure the quality and purity of the precursor isoprene. This was successfully achieved by cryogenically trapping lower volatility compounds such as monoterpenes before isoprene was introduced into the CLOUD chamber.

1 Introduction

Emissions of biogenic volatile organic compounds (BVOCs) impact the oxidation capacity of the atmosphere and serve as precursors for secondary organic aerosols (SOA) (Hallquist et al., 2009) through the formation of low-volatility oxidation products. They are emitted by a large variety of vegetation (~ 1150 Tg C yr^{-1}). The most abundantly emitted BVOCs on a global scale are isoprene (70 %) and monoterpenes (11 %) (Guenther et al., 2012). These BVOCs serve as main gas phase precursors for lower volatility oxidation products that play a crucial role for secondary organic aerosol (SOA) formation, and have been also related to new particle formation (NPF) over forest regions in the presence of sulfuric acid (Hallar et al., 2011; Held et al., 2004; Pierce et al., 2014; Pryor et al., 2010; Riipinen et al., 2007; Yu et al., 2014). While their contribution

to the global carbon budget is well established in general, too little is known about the contribution of different BVOC species to NPF.

The role of monoterpenes, especially α-pinene, has been extensively studied in this context. Recent studies suggest that NPF proceeds via highly oxidised low volatility organic compounds that are formed through autoxidation reactions of peroxy radicals from α-pinene ozonolysis. The formation of the clusters necessary for NPF can occur in the presence of sulfuric acid, as well as in its absence (Ehn et al., 2014; Kirkby et al., 2016; Kulmala et al., 2013; Schobesberger et al., 2013; Riccobono et al., 2014; Winkler et al., 2012).

Despite being the most dominant BVOC on a global scale (Guenther et al., 2012) the role of isoprene in NPF is far less understood compared to monoterpenes. The importance of isoprene oxidation products for aerosol formation has been shown in laboratory studies (Claeys et al., 2004; Kroll and Seinfeld, 2008). Products from oxidation with OH radicals (e.g. isoprene epoxydiols (IEPOX)) can actively partition into atmospheric aerosol particles to form SOA (Lin et al., 2013, L. Xu et al., 2015). Epoxides have recently been shown in laboratory studies to contribute to the growth of sulfuric acid particles in the 4 – 10 nm range at low relative humidity (W. Xu et al., 2014). However, based on the observed suppression of biogenic NPF in the presence of isoprene in plant chamber studies, Kiendler-Scharr et al. (2009) proposed a chemical mechanism that is based on OH depletion by isoprene itself to explain the observed suppression of NPF, and suggested that the suppression effect depends on the concentration ratio (R) of isoprene carbon to monoterpene carbon. While this mechanism may be reasonable in a well-controlled chamber environment with relatively simple chemical processes, especially in terms of HO_x and NO_x chemistry, it is not plausible for real forests. Numerous field studies and atmospheric observations have detected no reduction in OH radical concentration caused by isoprene or any other BVOC (Lelieveld et al., 2008). Even though OH radical concentrations are not reduced by isoprene, a suppression of NPF is observed in isoprene-dominant forests as a recent summertime field study (SOAS) undertaken in Alabama (southeast of US), Lee et al. (2016) has shown, where the smallest particles do not grow in isoprene-dominated environments despite apparently favourable chemical precursor conditions. A prominent example is the Amazon rainforest ($R \sim 15$) where extensive and continuous aerosol measurements have been conducted over the last decades. These measurements show a consistent lack of NPF at forest sites (Pöhlker et al., 2012) as well as sites influenced by biomass-burning (Rissler et al., 2006). The goal of these studies, however, was not to investigate the chemical mechanism behind the occurring suppression of NPF in the Amazon rainforest. Besides the Amazon, other studies have also reported the absence of NPF in several isoprene dominant forests across the United States (Kanawade et al., 2011; Bae et al., 2010; Pillai et al., 2013; Hallar et al., 2016; Yu et al., 2015). The R values observed during SOAS were between 1 and 10, within the range of other R values from forest with a reported lack of NPF in summertime. In the boreal forests in Hyytiäla, Finland on the other hand, the R value was only ~0.18 and NPF was frequently observed.

The simple algorithms of current climate models predict NPF with nucleation rates independent of the R value since they only take the total sum of low-volatility organic compounds into account, without regard to their actual composition in forests (Kirkby et al., 2011: Riccobono et al., 2014). As Lee et al. (20016) have demonstrated it is not feasible to simply apply current biogenic NPF knowledge to isoprene-dominant forests because it is derived solely from laboratory experiments

of pure monoterpene oxidation. At present it is still unclear how the oxidation products from isoprene may alter the oxidation chemistry of terpenes and in turn affect NPF in mixed forest environments. Further studies on this subject are required to improve our understanding.

During isoprene NPF studies at the CLOUD chamber, we detected unexpected ion signals at m/z = 137.133 ($C_{10}H_{17}^+$) and

5   m/z = 81.070 ($C_6H_9^+$), besides the expected protonated isoprene, with the recently developed high resolution proton transfer reaction time-of-flight mass spectrometer (PTR3-TOF, Breitenlechner et al., 2017). Here we will explain and discuss the origin and the impact of these ion signals.

2 Experimental

2.1 Instrumentation

10   **2.1.1 PTR3**

In the present study we used a novel PTR3, a proton transfer reaction-time-of-flight mass spectrometer (PTR-TOF) utilising a new gas inlet and an innovative reaction chamber design, that is described in detail in (Breitenlechner et al., 2017). The new reaction chamber consists of a tripole operated with rf voltages generating an electric field only in the radial direction. An elevated electrical field is necessary to reduce clustering of primary hydronium (H_3O^+) and product ions with water

15   molecules present in the sample gas. The PTR3 was operated at 80 mbar pressure, and a constant temperature of 38 °C in the tripole reaction chamber. The rf amplitude was adjusted to 700-800 V_{p-p}, which corresponds to an E/N of typically 95 Td (E, electric field strength; N, number gas density of air in the drift tube; unit, Townsend, Td; 1 Td = 10^{-17} V cm^2). During CLOUD 10 (autumn 2015) and CLOUD 11 (autumn 2016) campaigns the PTR3 was regularly calibrated. For this purpose, known concentrations of isoprene and α-pinene from a gas standard were diluted in 1 slpm zero air. Calibrations were

20   performed for typical operating conditions of the CLOUD chamber: 38 % and 85 % relative humidity at 5 °C, respectively. The instrumental background signal was determined by measuring chamber zero air. PTR3 raw data have been processed using newly developed software capable of high resolution and multipeak analysis as described in Breitenlechner et al., 2017. Processed data were duty cycle corrected ($Dcps, (i) = Cps(i) * \sqrt{101/m_i}$) which compensates for mass-dependent transmission of the TOF mass spectrometer.

25   **2.1.2 CI-APi-ToF**

The Chemical Ionisation Atmospheric Pressure Interface Time of Flight mass spectrometer (nitrate-CI-API-TOF, Tofwerk AG, Thun, Switzerland) uses an ion source similar to the design of Eisele and Tanner (1993) although, instead of a radioactive source, a corona discharge is used to generate nitrate primary ions $NO_3^-(HNO_3)_{0-2}$ (Kürten et al., 2011). The instrument was calibrated with respect to sulfuric acid (Kürten et al., 2012), and for the mass dependent transmission

efficiency (Heinritzi et al., 2016). For detailed information on the quantification of highly oxygenated organic molecules, the reader is referred to Kirkby et al. (2016).

2.1.3 Cryotrap

A cryotrap was added to the isoprene gas supply line directly behind the gas bottle to freeze possible contaminations with lower volatility out and effectively remove impurity compounds like monoterpenes or higher oxidised organics. The cryotrap consisted of a chiller coil placed inside a 100 mm diameter dewar flask filled with Huber DW-Therm thermofluid. The chiller maintained the liquid at -57.6 °C. Surrounding the chiller coil and immersed in the dewar liquid was a second spiral coil with six rings of 85 mm diameter through which the gas passed straight from the isoprene bottle (max. flow 10 sccm, average flow rate 5 sccm). The dewar flask was positioned upstream of the isoprene mass flow controller (MFCs). The isoprene coil was 6/4 mm diameter (OD/ID) electropolished stainless steel, and was thoroughly cleaned before use. The total length of the gas pipe inside the dewar flask was approximately 1.8 m. The cryotrap was in use for a total of 14 days measurement time.

2.2 Experimental procedures

2.2.1 Chamber experiments

Measurements were carried out in the CLOUD (Cosmics Leaving Outdoor Droplets) chamber at CERN (Duplissy et al., 2016; Kirkby et al., 2011) during the CLOUD 10 campaign in autumn 2015 and the CLOUD 11 campaign in autumn 2016. During nucleation studies of pure isoprene over the course of the CLOUD 10 campaign in 2015, 13.5 ppbv of isoprene (1 % isoprene in N_2, purity 99 %, CHARBAGAS AG) were introduced into the chamber. Ozone (45 ppbv) was introduced approximately 10 hours after conditioning the chamber in two steps for additional 9.5 hours. The experiment was carried out at 85 % relative humidity and 5 °C. Additional experiments were conducted during the CLOUD 11 campaign in 2016, this time with a cryotrap added to the isoprene supply line. For this purpose, 33.5 ppbv of isoprene were injected into the chamber, and ozone (35 ppbv) was added 5 hours later. After a reaction time of 5.5 hours the cryotrap was activated to remove low volatility contaminants and measurements continued for another 4 hours. This experiment was carried out at 37 % relative humidity and 6 °C. Gas phase precursors were measured with the PTR3-TOF. Simultaneously, a nitrate chemical-ionisation atmospheric-pressure-interface time-of-flight (CI-API-TOF) mass spectrometer was used to analyse the highly oxygenated organic compounds from ozonolysis experiments.

2.2.2 Cryotrap evaporation experiment

After a total of two weeks of operation, the cryotrap was disconnected from the chamber system and directly connected to the PTR3 inlet. A steady stream of dry N_2 (3 slpm) was fed through the isoprene coil. After a baseline determination, the spiral coil was removed from the chiller liquid and allowed to warm up from -57.6 °C to room temperature over a period of

three hours. The concentrations of released organic compounds were measured with the PTR3. After 45 min. an additional 1:2 dilution with dry N_2 became necessary due to a rapid depletion of primary ions.

3 Result and discussion

Figure 1a shows the temporal behaviour of the ion signals at $m/z = 69.070$ ($C_5H_9^+$) and $m/z = 41.039$ ($C_3H_5^+$), corresponding

5 to protonated isoprene and its fragment, during the 2016 experiment. After isoprene concentrations reached a steady level of ~33.5 ppbv, ozone (~35 ppbv) was continuously injected, and the cryotrap was switched on after several hours of oxidation to freeze out possible low volatility contaminants whose presence was suspected in 2015. As expected, the ion signals at $m/z = 69.070$ and $m/z = 41.039$ were linearly correlated over the entire course of the experiment, independent of experimental conditions, consistent with fragment formation inside the PTR3 instrument (Fig. 1b).

10 We observed additional ion signals at $m/z = 137.133$ ($C_{10}H_{17}^+$) and $m/z = 81.070$ ($C_6H_9^+$) when isoprene was added. These ion signals correspond to typical mass-to-charge ratios of protonated monoterpenes and the corresponding fragment ion. Contrary to the isoprene signal, the ion signals at both $m/z = 137.133$ and $m/z = 81.070$ show dependence on ozone, and a decrease induced by the cryotrap. Using the sensitivity of the α-pinene calibration, about 1 ppbv of α-pinene or monoterpene analogues were observed. This amount is equivalent to 3 % of the measured isoprene (33.5 ppbv). Correlation of

15 $m/z = 81.070$ and $m/z = 137.133$ shows two slopes, which, in turn, hints at two various sources for the $C_{10}H_{17}^+$ signal observed with PTR3 (Fig. 1c).

We explain the formation of the "monoterpene" signal, on one hand, with secondary association reactions of protonated isoprene with isoprene within the PTR3 reaction chamber forming $C_{10}H_{17}^+$ ions. As will be shown below, this route accounts for two-thirds of the total signal detected at $m/z = 137.133$, which is equivalent to 2% relative to the isoprene signal. On the

20 other hand, one-third of the total $C_{10}H_{17}^+$ signal or 1% (relative to isoprene) is caused by dimerization of isoprene inside the gas bottle to form [4+2] cycloaddition products. The amount of dimerization inside the gas bottle was estimated from a chamber experiment during which the cryotrap was switched off at the beginning, and then turned on for the last hours of measurement. The cycloaddition product is equal to the difference, Δ, between the maximum concentration before ozone injection and the decrease due to oxidation by ozone and freeze-out caused by the cryotrap (Fig. 1a).

25 ### 3.1 Secondary association reactions within the PTR3 reaction chamber

Figure 2a shows the temporal behaviour of the ion signals at $m/z = 137.133$ ($C_{10}H_{17}^+$), $m/z = 81.070$ ($C_6H_9^+$) and $m/z = 273.258$ ($C_{20}H_{33}^+$) monitored during the warm-up of the cryotrap during an experiment at the end of the 2016 campaign after two weeks of freezing out the low volatility impurities of the isoprene. Immediately after removal of the spiral coil from the cooling liquid, we observed signals at all three mass-to-charge ratios. At first glance their temporal

30 behaviour seems to be identical, but a closer look at the correlations reveals significant differences. The protonated monoterpene at $m/z = 137.133$ and its fragment at $m/z = 81.070$ show a linear dependency (Fig. 2b), which is expected from

ion fragmentation within the PTR3-TOF following pseudo first order kinetics between $H_3O^+ \bullet (H_2O)_n$ (n=0-2) primary ions in reactions with the reactant $C_{10}H_{16}$ (1).

$$H_3O^+(H_2O)_n + C_{10}H_{16} \rightarrow C_{10}H_{17}^+ + (n+1)\,H_2O \qquad (1a)$$

$$\rightarrow C_6H_9^+ + C_4H_8 + (n+1)\,H_2O \qquad (1b)$$
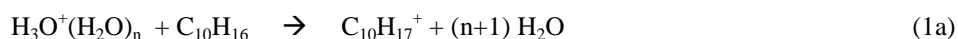
Comparison of $m/z = 137.133$ and $m/z = 273.258$, however, reveals a quadratic dependency (Fig. 2c) and indicates that $C_{20}H_{33}^+$ is the product of the secondary association reaction of $C_{10}H_{17}^+$ with $C_{10}H_{16}$ in the PTR3 reaction chamber (2).

$$C_{10}H_{17}^+ + C_{10}H_{16}\ (+M) \rightarrow C_{10}H_{17}^+(C_{10}H_{16}) + M \qquad (2)$$

Contrary to a classical proton-transfer-reaction time-of-flight mass spectrometer (PTR-TOF-MS) (Graus et al. 2010), the PTR3 operates at a much higher drift pressure (80 mbar) and at a longer reaction time (3 ms). This leads to a strong increase in ion molecule collisions inside the reaction zone of the PTR3 which enables secondary association reactions to become visible at reactant concentrations at about 10 ppbv compared to 10 ppmv in classical PTR-MS (Hansel et al. 1995).

The results shown in Figure 2 demonstrate that monoterpene like compound are released from the spiral coil during warm-up. This means that monoterpenes were present in the isoprene gas bottle.

In Figure 3 we compare the correlation of $m/z = 137.133$ with $m/z = 69.070$ (Fig. 3a and 3c) obtained during chamber experiments 2016 without cryotrap and before ozone injection and the correlation of $m/z = 273.258$ with $m/z = 137.133$ (Fig. 3b and 3d) obtained during cryotrap evaporation experiments in 2016. While the correlations of $m/z = 273.258$ with $m/z = 137.133$ in Fig. 3b and 3d show a clear quadratic dependence, the correlation of $m/z = 137.133$ with $m/z = 69.070$ in Fig. 3a seems to indicate two overlapping processes: a quadratic one from the secondary association reaction and an additional linear process. A closer look at the lower concentration range where secondary association reaction isn't yet dominant reveals that this is indeed the case (Fig. 3c). Therefore, we identify two processes that create the observed signal at $m/z = 137.133$:

- *Secondary association reaction within the PTR3 reaction chamber*

$$H_3O^+ \bullet (H_2O)_n + C_5H_8 \longrightarrow C_5H_9^+ + (n+1)H_2O \qquad (3a)$$

$$C_5H_9^+ + C_5H_8 + M \longrightarrow C_{10}H_{17}^+ + M \qquad (3b)$$
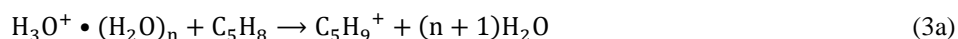
- *Direct ionisation of a C_{10} precursor*

$$H_3O^+ \bullet (H_2O)_n + C_{10}H_{16} \longrightarrow C_{10}H_{17}^+ + (n+1)H_2O \qquad (4)$$
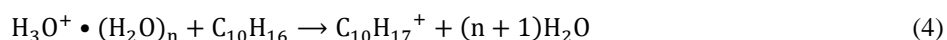
3.2 Dimerization inside the gas bottle

Dimerization of pure isoprene is known to occur when stored without a stabiliser (0.000017 % per hour at 20 °C, Estevez et al., 2014 and reference therein). It is influenced by pressure and temperature and proceeds via a [4+2] cycloaddition with isoprene acting both as diene and dienophile. This reaction can explain the observed compound at $m/z = 137.133$ and $m/z = 81.070$ ($C_6H_9^+$). Cycloaddition of isoprene has been well documented (Citroni et al., 2007; Compton et al., 1976;

Estevez et al., 2014; Groves and Lehrle, 1992; Walling and Peisach, 1958), and thermally-induced polymerisation in the gas phase has recently been shown for heated GC-inlets. The dimerization leads predominantly to six-membered rings, mainly the [4+2] Diels-Alder products sylvestrene and limonene (Estevez et al., 2014 and references therein). This known dimerization is the reason for the addition of *p*-tert-butyl catechol (TBC) as a stabiliser to liquid isoprene (Sigma Aldrich, 99 % purity, 139 ppm TBC for the used gas standard). Despite the addition of TBC as stabiliser to prevent polymerisation inside the gas bottle (stainless steel, 2 years old in 2017), 1 % of dimerized isoprene (~350 pptv) could be observed at $m/z = 137.133$ in 2016. The monoterpene analogues, presumably the favoured cycloaddition products sylvestrene and limonene (Wang et al., 2013), have much lower vapour pressures than isoprene and are, therefore, effectively removed from the system by the cryotrap (Fig. 1a). We found that the ratio between the total signal at $m/z = 137.133$ (sum of cycloaddition product from gas bottle and secondary ionic clusters) and isoprene changed between the autumn 2015 campaign (CLOUD 10) and the autumn 2016 campaign (CLOUD 11). It doubled over the course of a year, presumably due to a depletion of the stabiliser and increased dimerization of the isoprene precursor from 1.5 % to a total of 3 %.

3.3 Impact of impurities

Due to the presence of double bonds isoprene and especially monoterpenes show a high reactivity towards ozone. The reaction rate of *d*-limonene with ozone is even faster (21.1×10^{-17} cm^3 molecule^{-1} s^{-1}) than the corresponding reaction rate of α-pinene (9.4×10^{-17} cm^3 molecule^{-1} s^{-1}) and both are significantly faster than the one of isoprene (1.3×10^{-17} cm^3 molecule^{-1} s^{-1} at 298 K, Khamaganov and Hites, 2001). However, it is convenient to assume that the reaction rate of sylvestrene is also similar to that of limonene considering the structural similarity of limonene (methyl group in *meta*-position instead of *para*-position).

The impact of the different classes of oxidation products after ozone exposure and, more importantly, after the cryotrap freeze-out of the low volatility precursors was investigated during the 2016 CLOUD measurements. Oxidation products from isoprene ozonolysis are easily distinguishable from oxidation products of the monoterpene analogues. Isoprene ozonolysis products show a significant increase upon ozone exposure, but are not affected by the cryotrap due to the high vapour pressure of the precursor and continue to increase until reaching steady state concentrations (Fig. 4a). The lower vapour pressure of the monoterpene analogues that are present as impurities in the gas bottle, on the other hand, lead to a decrease in monoterpene oxidation products when frozen out by the cryotrap (Fig. 4b). Despite significantly lower concentrations of the low volatility precursor, at least one third of the more than 200 identified signals with $H_3O^+ \cdot (H_2O)_n$ as primary reagent ions (up to $m/z = 350$) show the behaviour of monoterpene oxidation products. The total raw signals for monoterpene oxidation products are smaller than for isoprene oxidation products but concentrations are still in the pptv range for a given injection of 33.5 ppbv of isoprene with 1 % of monoterpene contamination relative to isoprene concentrations.

The effect of the cryotrap on the oxidation product distribution was not only observed by means of PTR3 but also by means of CI-APi-TOF mass spectrometry. Figure 5 shows a mass defect plot comparing highly oxygenated molecules (HOMs) before and during the deployment of the cryotrap using CI-APi-TOF data from 2016. Unfortunately, steady state could not

be reached for the freeze-out of the monoterpene analogues, so monoterpene oxidation products remain visible. It takes 3 hours to exchange the gases in the CLOUD chamber meaning that after starting to completely remove the monoterpenes from the isoprene supply line 3 hours later 63% of the original steady state monoterpene concentration is still present. Nevertheless, the impact of the partial removal of the monoterpene like impurities is clearly visible. Reduction of the lower

5   volatility precursors leads to a general decrease in signal intensity, and complete disappearance of the heavier masses, especially in the mass to charge range of the C_{10} compounds, with $C_{10}H_{14}O_9$ being the predominant compound before freeze-out of the low volatility precursors. This clearly indicates a significant change in the observed oxidation products, and shows how strongly trace contaminations, even at low concentrations, can impact gas phase oxidation processes and the formation of HOMs from isoprene ozonolysis.

10   **4 Conclusion**

We have observed ion signals at *m/z* = 137.133 and *m/z* = 81.070 during presumably pure isoprene oxidation experiments which correspond to monoterpene signals. The sources of these signals were attributed to secondary association reaction between protonated isoprene and isoprene in the PTR3-TOF (two-thirds of total signal) and, more significantly, dimerization of isoprene inside the gas bottle (one third of total signal). Dimerization of isoprene leads to compounds identical to

15   monoterpenes in structure and chemical behaviour, and has a significant impact on chemical oxidation processes and gas phase composition. Despite comparatively low concentrations, these trace contaminations have a considerable impact on the distribution of HOMs from ozonolysis due to their fast reaction rates with ozone.

Therefore, it is essential to control the purity of the isoprene precursor. This can effectively be achieved either by use of freshly distilled isoprene preferably stored in a glass vial, or by use of a cryotrap to freeze out low volatility contaminants

20   which has successfully been demonstrated in this work.

Acknowledgements

We would like to thank CERN for supporting CLOUD with important technical and financial resources, and for providing a particle beam from the CERN Proton Synchrotron. We also thank Albin Wasem/CERN and Serge Mathot/CERN for designing and constructing the cryotrap. This research has received funding from the EC Seventh Framework Programme

25   (Marie Curie Initial Training Network "CLOUD-TRAIN" no. 316662).

References

Bae, M.-S., Schwab, J. J., Hogrefe, O., Frank, B. P., Lala, G. G., and Demerjian, K. L.: Characteristics of size distributions at urban and rural locations in New York, Atmos. Chem. Phys., 10, 4521–4535, doi:10.5194/acp-10-4521-2010, 2010.

Breitenlechner, M., Fischer, L., Hainer, M., Heinritzi, M., Curtius, J., and Hansel, A.: PTR3: An Instrument for Studying the Lifecycle of Reactive Organic Carbon in the Atmosphere, Analytical chemistry, 89, 5824–5831, doi:10.1021/acs.analchem.6b05110, 2017.

Citroni, M., Ceppatelli, M., Bini, R., and Schettino, V.: Dimerization and polymerization of isoprene at high pressures, The
5   journal of physical chemistry. B, 111, 3910–3917, doi:10.1021/jp0701993, 2007.

Claeys, M., Graham, B., Vas, G., Wang, W., Vermeylen, R., Pashynska, V., Cafmeyer, J., Guyon, P., Andreae, M. O., Artaxo, P., and Maenhaut, W.: Formation of secondary organic aerosols through photooxidation of isoprene, Science (New York, N.Y.), 303, 1173–1176, doi:10.1126/science.1092805, 2004.

Compton, D. A. C., George, W. O., and Maddams, W. F.: Conformations of conjugated hydrocarbons. Part 1. A
10   spectroscopic and thermodynamic study of buta-1,3-diene and 2-methylbuta-1,3-diene (isoprene), J. Chem. Soc., Perkin Trans. 2, 1666, doi:10.1039/p29760001666, 1976.

Duplissy, J., Merikanto, J., Franchin, A., Tsagkogeorgas, G., Kangasluoma, J., Wimmer, D., Vuollekoski, H., Schobesberger, S., Lehtipalo, K., Flagan, R. C., Brus, D., Donahue, N. M., Vehkamäki, H., Almeida, J., Amorim, A., Barmet, P., Bianchi, F., Breitenlechner, M., Dunne, E. M., Guida, R., Henschel, H., Junninen, H., Kirkby, J., Kürten, A.,
15   Kupc, A., Määttänen, A., Makhmutov, V., Mathot, S., Nieminen, T., Onnela, A., Praplan, A. P., Riccobono, F., Rondo, L., Steiner, G., Tome, A., Walther, H., Baltensperger, U., Carslaw, K. S., Dommen, J., Hansel, A., Petäjä, T., Sipilä, M., Stratmann, F., Vrtala, A., Wagner, P. E., Worsnop, D. R., Curtius, J., and Kulmala, M.: Effect of ions on sulfuric acid-water binary particle formation: 2. Experimental data and comparison with QC-normalized classical nucleation theory, J. Geophys. Res. Atmos., 121, 1752–1775, doi:10.1002/2015JD023539, 2016.

20   Ehn, M., Thornton, J. A., Kleist, E., Sipilä, M., Junninen, H., Pullinen, I., Springer, M., Rubach, F., Tillmann, R., Lee, B., Lopez-Hilfiker, F., Andres, S., Acir, I.-H., Rissanen, M., Jokinen, T., Schobesberger, S., Kangasluoma, J., Kontkanen, J., Nieminen, T., Kurtén, T., Nielsen, L. B., Jørgensen, S., Kjaergaard, H. G., Canagaratna, M., Maso, M. D., Berndt, T., Petäjä, T., Wahner, A., Kerminen, V.-M., Kulmala, M., Worsnop, D. R., Wildt, J., and Mentel, T. F.: A large source of low-volatility secondary organic aerosol, Nature, 506, 476–479, doi:10.1038/nature13032, 2014.

25   Eisele, F. L. and Tanner, D. J.: Measurement of the gas phase concentration of H 2 SO 4 and methane sulfonic acid and estimates of H 2 SO 4 production and loss in the atmosphere, J. Geophys. Res., 98, 9001–9010, doi:10.1029/93JD00031, 1993.

Estevez, Y., Gardrat, C., Berthelot, K., Grau, E., Jeso, B. de, Ouardad, S., and Peruch, F.: Unexpected dimerization of isoprene in a gas chromatography inlet. A study by gas chromatography/mass spectrometry coupling, Journal of
30   chromatography. A, 1331, 133–138, doi:10.1016/j.chroma.2014.01.035, 2014.

Groves, S. and Lehrle, R.: Dimerisation of isoprene in a mass spectrometer source in GC-MS analysis, Polymer Degradation and Stability, 38, 183–186, doi:10.1016/0141-3910(92)90112-I, 1992.

Guenther, A. B., Jiang, X., Heald, C. L., Sakulyanontvittaya, T., Duhl, T., Emmons, L. K., and Wang, X.: The Model of Emissions of Gases and Aerosols from Nature version 2.1 (MEGAN2.1): An extended and updated framework for modeling biogenic emissions, Geosci. Model Dev., 5, 1471–1492, doi:10.5194/gmd-5-1471-2012, 2012.

Hallar, A. G., Lowenthal, D. H., Chirokova, G., Borys, R. D., and Wiedinmyer, C.: Persistent daily new particle formation at a mountain-top location, Atmospheric Environment, 45, 4111–4115, doi:10.1016/j.atmosenv.2011.04.044, 2011.

Hallar, A. G., Petersen, R., McCubbin, I. B., Lowenthal, D., Lee, S., Andrews, E., and Yu, F.: Climatology of New Particle Formation and Corresponding Precursors at Storm Peak Laboratory, Aerosol Air Qual. Res., 16, 816–826, doi:10.4209/aaqr.2015.05.0341, 2016.

Hallquist, M., Wenger, J. C., Baltensperger, U., Rudich, Y., Simpson, D., Claeys, M., Dommen, J., Donahue, N. M., George, C., Goldstein, A. H., Hamilton, J. F., Herrmann, H., Hoffmann, T., Iinuma, Y., Jang, M., Jenkin, M. E., Jimenez, J. L., Kiendler-Scharr, A., Maenhaut, W., McFiggans, G., Mentel, T. F., Monod, A., Prévôt, A. S. H., Seinfeld, J. H., Surratt, J. D., Szmigielski, R., and Wildt, J.: The formation, properties and impact of secondary organic aerosol: Current and emerging issues, Atmos. Chem. Phys., 9, 5155–5236, doi:10.5194/acp-9-5155-2009, 2009.

Heinritzi, M., Simon, M., Steiner, G., Wagner, A. C., Kürten, A., Hansel, A., and Curtius, J.: Characterization of the mass-dependent transmission efficiency of a CIMS, Atmos. Meas. Tech., 9, 1449–1460, doi:10.5194/amt-9-1449-2016, 2016.

Held, A., Nowak, A., Birmili, W., Wiedensohler, A., Forkel, R., and Klemm, O.: Observations of particle formation and growth in a mountainous forest region in central Europe, J. Geophys. Res. Atmos., 109, 23,709, doi:10.1029/2004JD005346, 2004.

Kanawade, V. P., Jobson, B. T., Guenther, A. B., Erupe, M. E., Pressley, S. N., Tripathi, S. N., and Lee, S.-H.: Isoprene suppression of new particle formation in a mixed deciduous forest, Atmos. Chem. Phys., 11, 6013–6027, doi:10.5194/acp-11-6013-2011, 2011.

Khamaganov, V. G. and Hites, R. A.: Rate Constants for the Gas-Phase Reactions of Ozone with Isoprene, α- and β-Pinene, and Limonene as a Function of Temperature, J. Phys. Chem. A, 105, 815–822, doi:10.1021/jp002730z, 2001.

Kiendler-Scharr, A., Wildt, J., Dal Maso, M., Hohaus, T., Kleist, E., Mentel, T. F., Tillmann, R., Uerlings, R., Schurr, U., and Wahner, A.: New particle formation in forests inhibited by isoprene emissions, Nature, 461, 381–384, doi:10.1038/nature08292, 2009.

Kirkby, J., Curtius, J., Almeida, J., Dunne, E., Duplissy, J., Ehrhart, S., Franchin, A., Gagne, S., Ickes, L., Kürten, A., Kupc, A., Metzger, A., Riccobono, F., Rondo, L., Schobesberger, S., Tsagkogeorgas, G., Wimmer, D., Amorim, A., Bianchi, F., Breitenlechner, M., David, A., Dommen, J., Downard, A., Ehn, M., Flagan, R. C., Haider, S., Hansel, A., Hauser, D., Jud, W., Junninen, H., Kreissl, F., Kvashin, A., Laaksonen, A., Lehtipalo, K., Lima, J., Lovejoy, E. R., Makhmutov, V., Mathot, S., Mikkila, J., Minginette, P., Mogo, S., Nieminen, T., Onnela, A., Pereira, P., Petäjä, T., Schnitzhofer, R., Seinfeld, J. H., Sipilä, M., Stozhkov, Y., Stratmann, F., Tome, A., Vanhanen, J., Viisanen, Y., Vrtala, A., Wagner, P. E., Walther, H., Weingartner, E., Wex, H., Winkler, P. M., Carslaw, K. S., Worsnop, D. R., Baltensperger, U., and Kulmala,

M.: Role of sulphuric acid, ammonia and galactic cosmic rays in atmospheric aerosol nucleation, Nature, 476, 429–433, doi:10.1038/nature10343, 2011.

Kirkby, J., Duplissy, J., Sengupta, K., Frege, C., Gordon, H., Williamson, C., Heinritzi, M., Simon, M., Yan, C., Almeida, J., Tröstl, J., Nieminen, T., Ortega, I. K., Wagner, R., Adamov, A., Amorim, A., Bernhammer, A.-K., Bianchi, F.,

5 Breitenlechner, M., Brilke, S., Chen, X., Craven, J., Dias, A., Ehrhart, S., Flagan, R. C., Franchin, A., Fuchs, C., Guida, R., Hakala, J., Hoyle, C. R., Jokinen, T., Junninen, H., Kangasluoma, J., Kim, J., Krapf, M., Kürten, A., Laaksonen, A., Lehtipalo, K., Makhmutov, V., Mathot, S., Molteni, U., Onnela, A., Peräkylä, O., Piel, F., Petäjä, T., Praplan, A. P., Pringle, K., Rap, A., Richards, N. A. D., Riipinen, I., Rissanen, M. P., Rondo, L., Sarnela, N., Schobesberger, S., Scott, C. E., Seinfeld, J. H., Sipilä, M., Steiner, G., Stozhkov, Y., Stratmann, F., Tomé, A., Virtanen, A., Vogel, A. L., Wagner, A.

10 C., Wagner, P. E., Weingartner, E., Wimmer, D., Winkler, P. M., Ye, P., Zhang, X., Hansel, A., Dommen, J., Donahue, N. M., Worsnop, D. R., Baltensperger, U., Kulmala, M., Carslaw, K. S., and Curtius, J.: Ion-induced nucleation of pure biogenic particles, Nature, 533, 521–526, doi:10.1038/nature17953, 2016.

Kroll, J. H. and Seinfeld, J. H.: Chemistry of secondary organic aerosol: Formation and evolution of low-volatility organics in the atmosphere, Atmospheric Environment, 42, 3593–3624, doi:10.1016/j.atmosenv.2008.01.003, 2008.

15 Kulmala, M., Kontkanen, J., Junninen, H., Lehtipalo, K., Manninen, H. E., Nieminen, T., Petäjä, T., Sipilä, M., Schobesberger, S., Rantala, P., Franchin, A., Jokinen, T., Järvinen, E., Äijälä, M., Kangasluoma, J., Hakala, J., Aalto, P. P., Paasonen, P., Mikkilä, J., Vanhanen, J., Aalto, J., Hakola, H., Makkonen, U., Ruuskanen, T., Mauldin, R. L., Duplissy, J., Vehkamäki, H., Bäck, J., Kortelainen, A., Riipinen, I., Kurtén, T., Johnston, M. V., Smith, J. N., Ehn, M., Mentel, T. F., Lehtinen, K. E. J., Laaksonen, A., Kerminen, V.-M., and Worsnop, D. R.: Direct observations of atmospheric aerosol

20 nucleation, Science (New York, N.Y.), 339, 943–946, doi:10.1126/science.1227385, 2013.

Kürten, A., Rondo, L., Ehrhart, S., and Curtius, J.: Performance of a corona ion source for measurement of sulfuric acid by chemical ionization mass spectrometry, Atmos. Meas. Tech., 4, 437–443, doi:10.5194/amt-4-437-2011, 2011.

Kürten, A., Rondo, L., Ehrhart, S., and Curtius, J.: Calibration of a chemical ionization mass spectrometer for the measurement of gaseous sulfuric acid, The journal of physical chemistry. A, 116, 6375–6386, doi:10.1021/jp212123n,

25 2012.

Lee, S.-H., Uin, J., Guenther, A. B., Gouw, J. A. de, Yu, F., Nadykto, A. B., Herb, J., Ng, N. L., Koss, A., Brune, W. H., Baumann, K., Kanawade, V. P., Keutsch, F. N., Nenes, A., Olsen, K., Goldstein, A., and Ouyang, Q.: Isoprene suppression of new particle formation: Potential mechanisms and implications, J. Geophys. Res. Atmos., 121, 14,621-14,635, doi:10.1002/2016JD024844, 2016.

30 Lelieveld, J., Butler, T. M., Crowley, J. N., Dillon, T. J., Fischer, H., Ganzeveld, L., Harder, H., Lawrence, M. G., Martinez, M., Taraborrelli, D., and Williams, J.: Atmospheric oxidation capacity sustained by a tropical forest, Nature, 452, 737–740, doi:10.1038/nature06870, 2008.

Lin, Y.-H., Zhang, H., Pye, H. O. T., Zhang, Z., Marth, W. J., Park, S., Arashiro, M., Cui, T., Budisulistiorini, S. H., Sexton, K. G., Vizuete, W., Xie, Y., Luecken, D. J., Piletic, I. R., Edney, E. O., Bartolotti, L. J., Gold, A., and Surratt, J. D.:

Epoxide as a precursor to secondary organic aerosol formation from isoprene photooxidation in the presence of nitrogen oxides, Proceedings of the National Academy of Sciences of the United States of America, 110, 6718–6723, doi:10.1073/pnas.1221150110, 2013.

Pierce, J. R., Westervelt, D. M., Atwood, S. A., Barnes, E. A., and Leaitch, W. R.: New-particle formation, growth and climate-relevant particle production in Egbert, Canada: Analysis from 1 year of size-distribution observations, Atmos. Chem. Phys., 14, 8647–8663, doi:10.5194/acp-14-8647-2014, 2014.

Pillai, P., Khlystov, A., Walker, J., and Aneja, V.: Observation and Analysis of Particle Nucleation at a Forest Site in Southeastern US, Atmosphere, 4, 72–93, doi:10.3390/atmos4020072, 2013.

Pöhlker, C., Wiedemann, K. T., Sinha, B., Shiraiwa, M., Gunthe, S. S., Smith, M., Su, H., Artaxo, P., Chen, Q., Cheng, Y., Elbert, W., Gilles, M. K., Kilcoyne, A. L. D., Moffet, R. C., Weigand, M., Martin, S. T., Pöschl, U., and Andreae, M. O.: Biogenic potassium salt particles as seeds for secondary organic aerosol in the Amazon, Science (New York, N.Y.), 337, 1075–1078, doi:10.1126/science.1223264, 2012.

Pryor, S. C., Spaulding, A. M., and Barthelmie, R. J.: New particle formation in the Midwestern USA: Event characteristics, meteorological context and vertical profiles, Atmospheric Environment, 44, 4413–4425, doi:10.1016/j.atmosenv.2010.07.045, 2010.

Riccobono, F., Schobesberger, S., Scott, C. E., Dommen, J., Ortega, I. K., Rondo, L., Almeida, J., Amorim, A., Bianchi, F., Breitenlechner, M., David, A., Downard, A., Dunne, E. M., Duplissy, J., Ehrhart, S., Flagan, R. C., Franchin, A., Hansel, A., Junninen, H., Kajos, M., Keskinen, H., Kupc, A., Kürten, A., Kvashin, A. N., Laaksonen, A., Lehtipalo, K., Makhmutov, V., Mathot, S., Nieminen, T., Onnela, A., Petäjä, T., Praplan, A. P., Santos, F. D., Schallhart, S., Seinfeld, J. H., Sipilä, M., Spracklen, D. V., Stozhkov, Y., Stratmann, F., Tomé, A., Tsagkogeorgas, G., Vaattovaara, P., Viisanen, Y., Vrtala, A., Wagner, P. E., Weingartner, E., Wex, H., Wimmer, D., Carslaw, K. S., Curtius, J., Donahue, N. M., Kirkby, J., Kulmala, M., Worsnop, D. R., and Baltensperger, U.: Oxidation products of biogenic emissions contribute to nucleation of atmospheric particles, Science (New York, N.Y.), 344, 717–721, doi:10.1126/science.1243527, 2014.

Riipinen, I., Sihto, S.-L., Kulmala, M., Arnold, F., Dal Maso, M., Birmili, W., Saarnio, K., Teinilä, K., Kerminen, V.-M., Laaksonen, A., and Lehtinen, K. E. J.: Connections between atmospheric sulphuric acid and new particle formation during QUEST III–IV campaigns in Heidelberg and Hyytiälä, Atmos. Chem. Phys., 7, 1899–1914, doi:10.5194/acp-7-1899-2007, 2007.

Rissler, J., Vestin, A., Swietlicki, E., Fisch, G., Zhou, J., Artaxo, P., and Andreae, M. O.: Size distribution and hygroscopic properties of aerosol particles from dry-season biomass burning in Amazonia, Atmos. Chem. Phys., 6, 471–491, doi:10.5194/acp-6-471-2006, 2006.

Schobesberger, S., Junninen, H., Bianchi, F., Lönn, G., Ehn, M., Lehtipalo, K., Dommen, J., Ehrhart, S., Ortega, I. K., Franchin, A., Nieminen, T., Riccobono, F., Hutterli, M., Duplissy, J., Almeida, J., Amorim, A., Breitenlechner, M., Downard, A. J., Dunne, E. M., Flagan, R. C., Kajos, M., Keskinen, H., Kirkby, J., Kupc, A., Kürten, A., Kurtén, T., Laaksonen, A., Mathot, S., Onnela, A., Praplan, A. P., Rondo, L., Santos, F. D., Schallhart, S., Schnitzhofer, R., Sipilä,

M., Tomé, A., Tsagkogeorgas, G., Vehkamäki, H., Wimmer, D., Baltensperger, U., Carslaw, K. S., Curtius, J., Hansel, A., Petäjä, T., Kulmala, M., Donahue, N. M., and Worsnop, D. R.: Molecular understanding of atmospheric particle formation from sulfuric acid and large oxidized organic molecules, Proceedings of the National Academy of Sciences of the United States of America, 110, 17223–17228, doi:10.1073/pnas.1306973110, 2013.

5 Walling, C. and Peisach, J.: Organic Reactions Under High Pressure. IV. The Dimerization of Isoprene 1, J. Am. Chem. Soc., 80, 5819–5824, doi:10.1021/ja01554a058, 1958.

Winkler, P. M., Ortega, J., Karl, T., Cappellin, L., Friedli, H. R., Barsanti, K., McMurry, P. H., and Smith, J. N.: Identification of the biogenic compounds responsible for size-dependent nanoparticle growth, Geophys. Res. Lett., 39, 863, doi:10.1029/2012GL053253, 2012.

10 Xu, L., Guo, H., Boyd, C. M., Klein, M., Bougiatioti, A., Cerully, K. M., Hite, J. R., Isaacman-VanWertz, G., Kreisberg, N. M., Knote, C., Olson, K., Koss, A., Goldstein, A. H., Hering, S. V., Gouw, J. de, Baumann, K., Lee, S.-H., Nenes, A., Weber, R. J., and Ng, N. L.: Effects of anthropogenic emissions on aerosol formation from isoprene and monoterpenes in the southeastern United States, Proceedings of the National Academy of Sciences of the United States of America, 112, 37–42, doi:10.1073/pnas.1417609112, 2015.

15 Xu, W., Gomez-Hernandez, M., Guo, S., Secrest, J., Marrero-Ortiz, W., Zhang, A. L., and Zhang, R.: Acid-catalyzed reactions of epoxides for atmospheric nanoparticle growth, J. Am. Chem. Soc., 136, 15477–15480, doi:10.1021/ja508989a, 2014.

Yu, F., Luo, G., Pryor, S. C., Pillai, P. R., Lee, S. H., Ortega, J., Schwab, J. J., Hallar, A. G., Leaitch, W. R., Aneja, V. P., Smith, J. N., Walker, J. T., Hogrefe, O., and Demerjian, K. L.: Spring and summer contrast in new particle formation over
20 nine forest areas in North America, Atmos. Chem. Phys., 15, 13993–14003, doi:10.5194/acp-15-13993-2015, 2015.

Yu, H., Ortega, J., Smith, J. N., Guenther, A. B., Kanawade, V. P., You, Y., Liu, Y., Hosman, K., Karl, T., Seco, R., Geron, C., Pallardy, S. G., Gu, L., Mikkilä, J., and Lee, S.-H.: New Particle Formation and Growth in an Isoprene-Dominated Ozark Forest: From Sub-5 nm to CCN-Active Sizes, Aerosol Science and Technology, 48, 1285–1298, doi:10.1080/02786826.2014.984801, 2014.

25
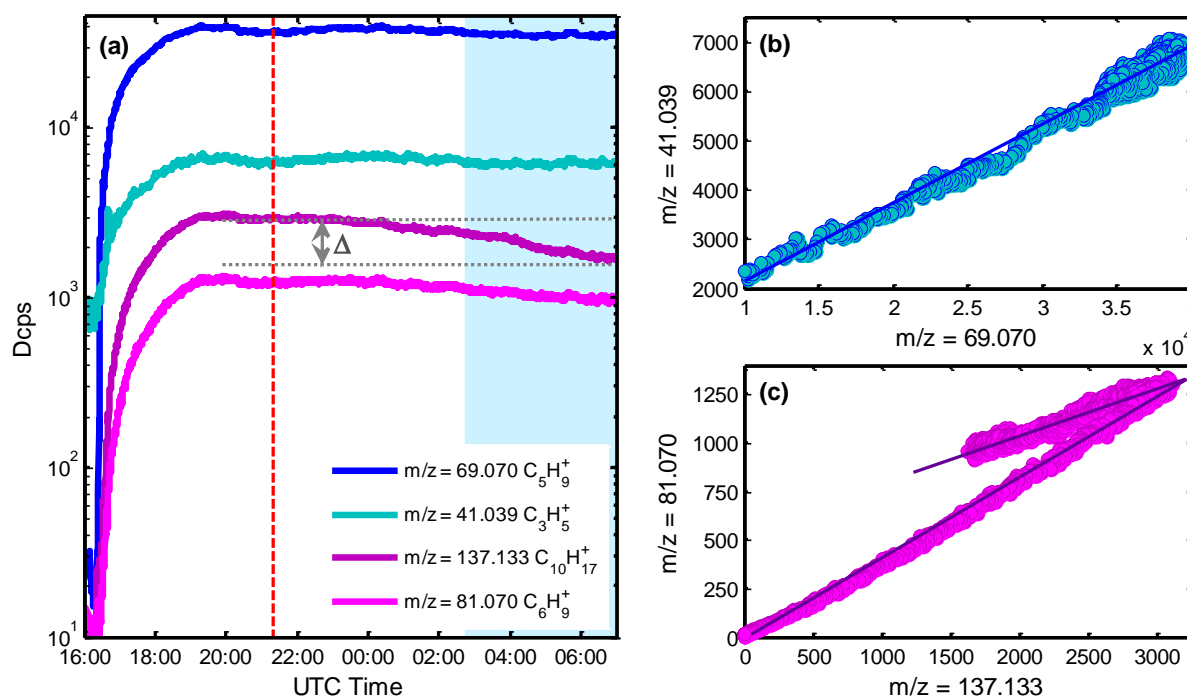
Figure 1: a) Time series of isoprene observed at the protonated mass *m/z* = 69.070, its main fragment at *m/z* = 41.039, isoprene cluster/monoterpene (*m/z* = 137.133) and their main fragment (*m/z* = 81.070) during the 2016 experiment. The blue shaded area corresponds to times with the cryotrap switched on, the dashed red line indicates the start of O$_3$, Δ marks the signal loss caused by ozonolysis and cryotrap freeze-out. **b)** Correlation plot of *m/z* = 69.070 and its main fragment *m/z* = 41.039, **c)** correlation plot of *m/z* = 137.133 and its main fragment *m/z* = 81.070.
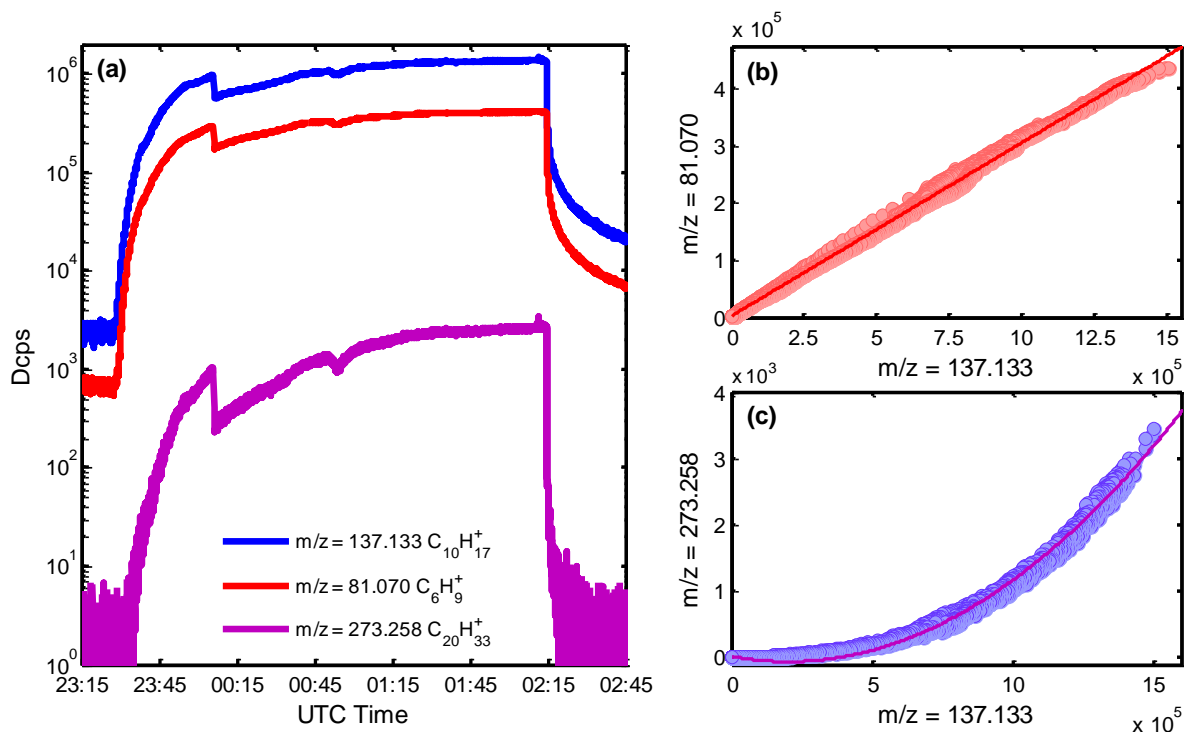
Figure 2: a) Time series of $m/z = 137.133$ **(C$_{10}$H$_{17}^+$),** $m/z = 81.070$ **(C$_6$H$_9^+$) and** $m/z = 273.258$ **(C$_{20}$H$_{33}^+$) during cryotrap evaporation experiment (2016), b) correlation plot of** $m/z = 137.133$ **(C$_{10}$H$_{17}^+$) and its main fragment** $m/z = 81.070$ **(C$_6$H$_9^+$), c) correlation plot of** $m/z = 137.133$ **(C$_{10}$H$_{17}^+$) and the secondary ionic cluster** $m/z = 273.258$ **(C$_{20}$H$_{33}^+$).**
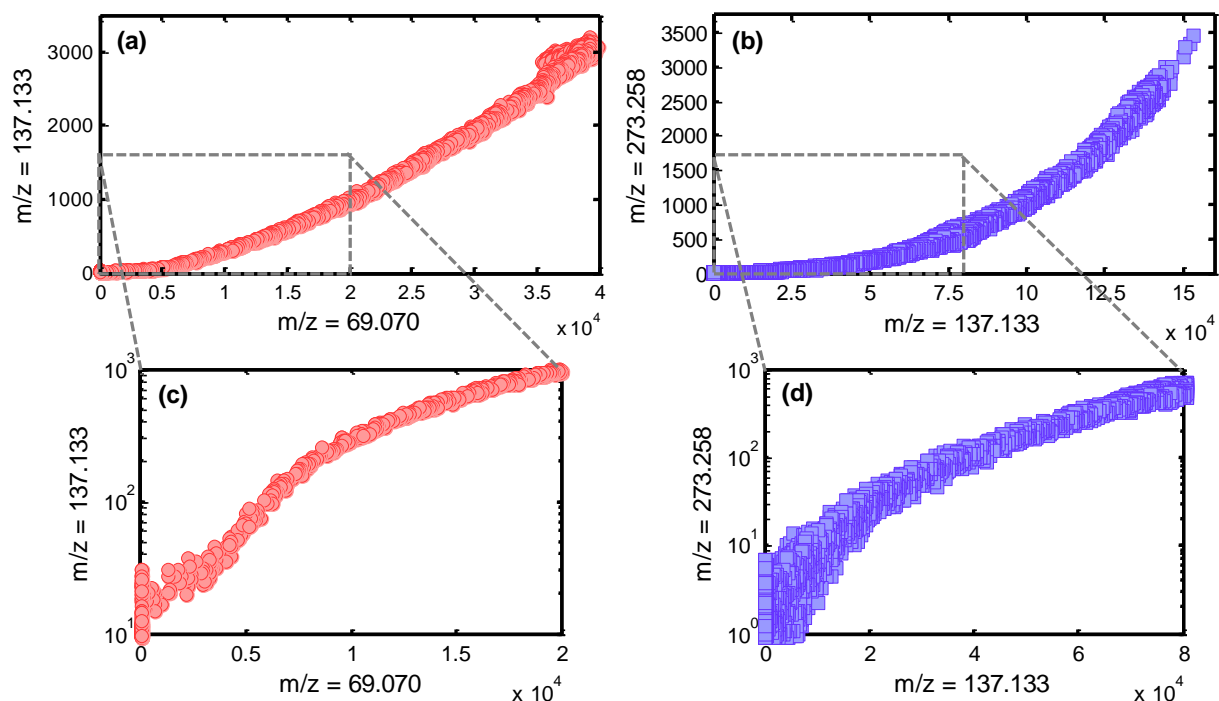
Figure 3: Comparison of the correlation plots of the 2016 chamber experiment (a) and 2016 evaporation experiment (b) for m/z = 69.070 vs. m/z = 137.133 (red) and m/z = 137.133 vs. m/z = 273.258 (purple). Panels a) shows the correlation over the initial chamber experiment without cryotrap and before the addition of ozone, panel b) shows the correlation over the entire evaporation experiment, panels c) and d) focus on the lower concentration range. For the pure secondary association reaction (b,d) a clear quadratic dependency is observed, while for the chamber experiment (a,c) two overlapping processes – especially in the lower concentration regime – take place before the cluster formation becomes the dominant pathway at higher concentrations.
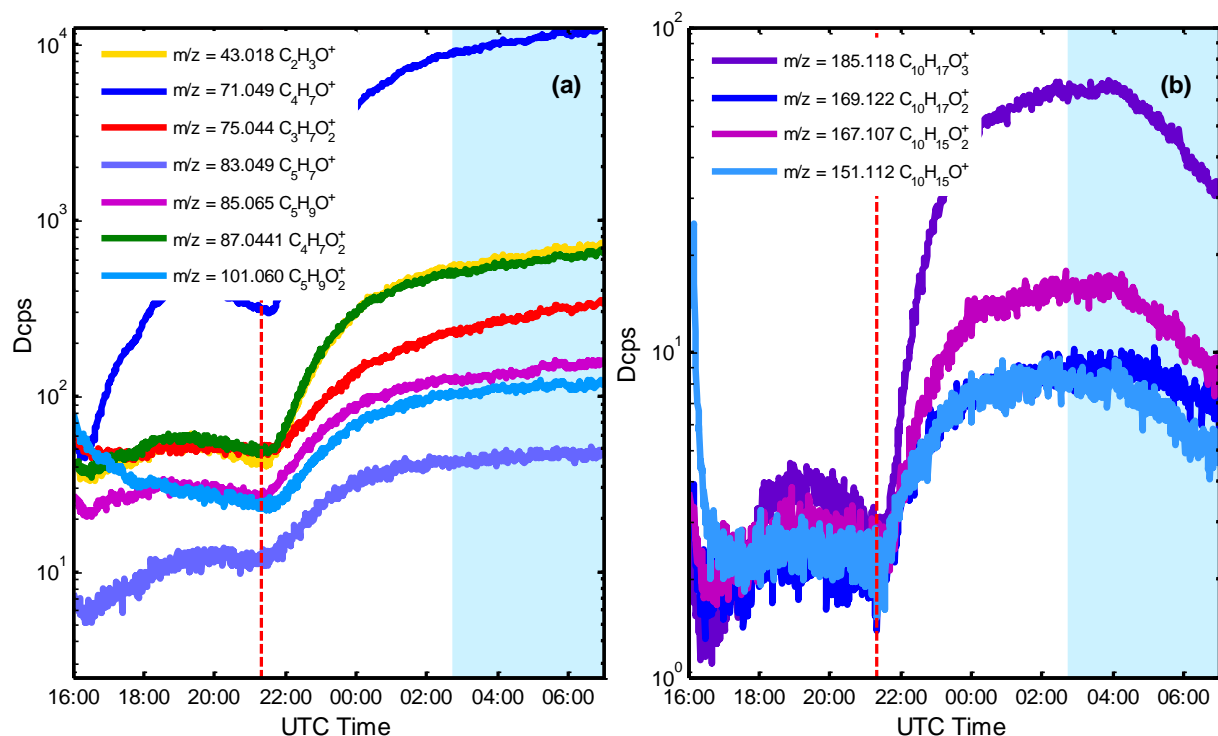
Figure 4: a) Time series of selected pure isoprene oxidation products in 2016, b) time series of main monoterpene-analogue oxidation products which show a typical decrease towards the end due to a removal of the precursor with the cryotrap while the isoprene products are not affected. The red line corresponds to the injection time of ozone and the blue shaded area to the times with cryotrap.
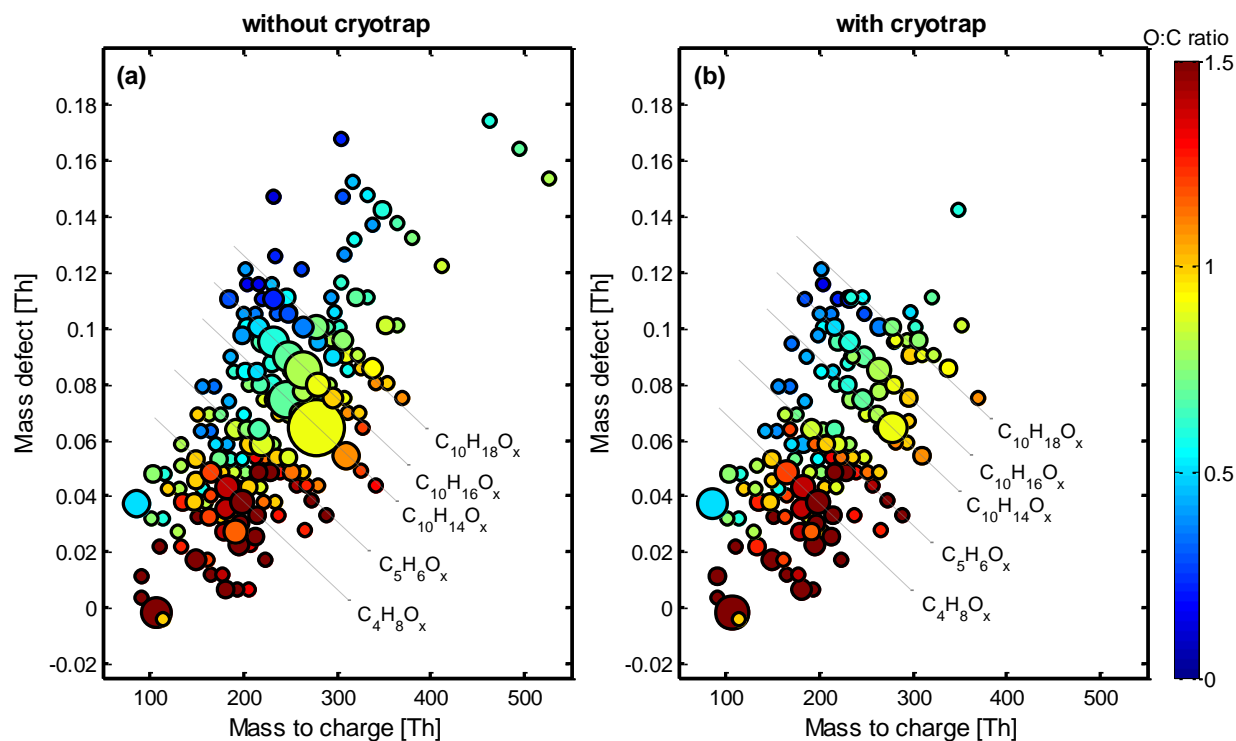
Figure 5: Mass defect plot obtained from 2016 CI-APi-ToF data after subtraction of primary ions ($NO_3^-(HNO_3)_{0-2}$) for a) isoprene ozonolysis without cryotrap and b) isoprene ozonolysis with cryotrap. The circle size corresponds to the signal intensity. Steady state was not reached for the measurements with cryotrap therefore cryogenic removal was incomplete and oxidation products from the monoterpene oxidation are still visible. Nevertheless, a significant decrease in signal intensities, especially in the C_{10} range, can be observed.